Latent heating rate profiles at different tropical cyclone stages during 2008 Tropical Cyclone Structure experiment: Comparison of ELDORA and TRMM PR retrievals

Myung-Sook Park, Russell L. Elsberry and Michael M. Bell

Department of Meteorology, Naval Postgraduate School, Monterey, California, USA

1. Introduction and methodology

Tropical cyclone formation involves dynamic processes on the synoptic scale, mesoscale and the convective scale. In the western North Pacific, the pre-tropical cyclone seedling may be a monsoon depression, tropical easterly waves, or tropical upper-tropospheric trough cell. It is hypothesized that the primary differences between developing and non-developing tropical cyclone seedling circulations occur in dynamic response to mesoscale convective system embedded in the pre-seedling circulation. For this upscale process, the mesoscale latent heating profile is a key factor to understand.

Recently, the airborne Electra Doppler Radar (ELDORA) has provided a unique observational tool to study hypotheses for mesoscale contributions to tropical cyclone formations. During Tropical Cyclone Structure (TCS)-08 field experiment, three-dimensional circulations and reflectivities of convection were observed by ELDORA on the mesoscale and convective scale (horizontal resolution as fine as 0.5–1 km) within 21 tropical cyclone circulations. Roux et al. (1993) show that the latent heating rate can be derived from the observed dynamics and hydrometeors by solving an analeastic form of the momentum equations and continuity equations of hydrometeors for a given environmental sounding. In this study, the latent heating rates from the ELDORA observations are derived for six missions into TCS-08 tropical circulations that were nearly coincident with the TRMM Precipitation Radar (PR) observations in space and time (Table 1; Fig. 1). The PR Spectral Latent Heating (SLH) algorithm of Shige et al. (2007), which converts the PR rain profile to latent heating rate via look-up table derived from simulations by cloud resolving model for each rain type classification, is compared with the in situ ELDORA profiles. The cases include an eyewall and an outer rainband of the mature stage in a Super Typhoon Jangmi prior to its peak intensity (Case I) and an outer rainband in Typhoon Sinlaku as it was beginning extratropical transition in extra-tropical coast (Case II), one case with convective regions in pre-tropical depression Nuri (Case III), and the case with a convective burst prior to Typhoon Sinlaku re-intensification (Case IV), and two tropical disturbances that never developed (Case IV and Case V).

The first objective of this study is to verify the statistical changes of the ELDORA-derived latent heating rates between mature, developing, and non-developing stages of tropical cyclone circulation. The structure changes in the ELDORA derived latent heating rate are then compared with those with the TRMM PR SLH algorithm. Comparison of the two latent heating rate data sets is primarily based on Contoured Frequency Altitude Diagrams (CFADs) for the two latent heating rate profiles. It this properly validated, the TRMM latent heating rate profiles can then be used to examine a very large sample of

developing and non-developing pre-tropical cyclone seedling systems during 12 years that TRMM has overpassed.

Table 1. Six cases with ELDORA observations during the TCS-08 experiment in various stages of tropical cyclone (TC).

TC circulation stages	Case number and name	ELDORA analysis lag		PR correlated	
		Date	Time (UTC)	Date	Time (UTC)
Mature	Case I TY Jangmi_Rb	9/26	2320−2340	9/26	2000
			2350−0000		
		9/27	0000−0010		
	Case II TY Sinlaku_Rb	9/19	0218−0230	9/18	2048
Developing	Case III (N) Pre-Nuri-Ncb	8/16	0000−0300	8/16	7:00
			0030−0100		
	Case III (S) Pre-Nuri-Scb		0315−0325		
			0325−0345		
	Case IV Pre-late Sinlaku	9/17	0140−0200	9/16	17:00
Non-Developing	Case V TCS25	8/29	0300−0330	8/29	08:10
	Case VI TCS51	10/3	0000-0030	10/3	06:43

Case I : Super Typhoon Jangmi

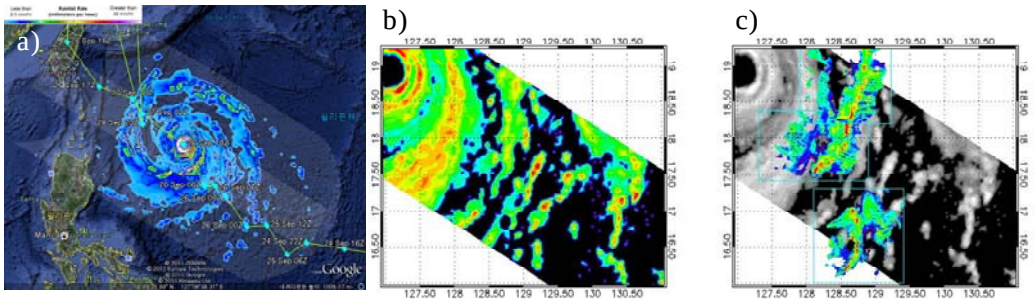

Figure 1. TRMM and aircraft plain views into the Case I. Left panels show the polar-orbiting (a) TRMM satellite PR rain rates on the narrow swath (215 km) at the observation time in Case I in Table 1 overlaid with the TRMM TMI on its wider swath (750 km) and the MTSAT infrared imagery. (b) PR reflectivities at 4 km height and (c) the corresponding ELDORA reflectivities at the same time.

2. **Summary of results**

a. Structure changes in the ELDORA latent heating rate during tropical cyclone life cycle

The ELDORA latent heating rate distributions demonstrate some physically reasonable differences in the outer rainbands in the Case I Jangmi and Case II Sinlaku that is beginning extratropical transition (Fig. 2). Whereas two mature cases both have low-level cooling maxima, the latent heating maximum is in lower levels for Case I and in upper levels for Case II. The ELDORA reflectivity and vertical profile of vertical wind (not shown) demonstrate that the convective and stratiform precipitation correspond well with the differences in the statistical structure changes of latent heating rate profiles. In particular, convective cells in the Case I TY Jangmi_Rb tend to be vertically erect with strong radar echoes with maximum reflectivity ~ 48 dBZ. Thus, high density of large hydrometeors produce a strong echo at lower levels consistent with cloud microphysical phase changes of vapor to water particles, and this induces low-level, strong condensational heating. In contrast, the convective cells in the outer rainband of Sinlaku have weaker radar echoes (maximum reflectivity ~ 35 dBZ), and are extremely tilted radially outward. Since Sinlaku at this time is approaching the southern coast of Japan, warm air to west is being lifted over cold air, which leads to a different latent heating distribution in the vertical in that in Jangmi .

The prominent differences in the CFADs for the pre-tropical depression Nuri developing stage Case III Pre-Nuri Scb and the TCS-25 non-developing disturbance Case V is that the magnitudes of latent heating and cooling rates in low levels around 3.5 km for the developing (non-developing) cases are non-symmetric (symmetric). That is, latent heating in Case III Pre-Nuri Scb exceeds 40 K h^{-1} but the cooling maximum has much lower values of −25 K h^{-1}. This decrease in evaporative cooling in the southern convective region that became Nuri is attributed to the more moist environment in the westerly wind environment compared to the northern convective region (Case III Pre-Nuri Scb) associated with the pre-existing easterly wave that did not developed.

Case IV pre-rein-Sinlaku, which is categorized as a developing stage, also has non-symmetric values of positive and negative latent heating rates. In particular, the maximum heating is as high as 80 K h^{-1} but maximum cooling is −50 K h^{-1}. This heating maximum in upper levels around 9 km in the pre-re-intensification stage of late Sinlaku is an indication that significant precipitation is occurring in the stratiform region of the very deep (~17 km) MCS, which is evident both in the satellite infrared imagery and ELDORA reflectivity observations. This intense MCS is to the east of the residual center of Typhoon Sinlaku in a region of strong vertical shear, so the MCS also has a large cooling rate at low levels. Thus, the difference between developing and non-developing cases is not just a shift in the level of maximum latent heating, but also involves decreases in evaporative cooling.

b. Comparison of the ELDORA and the PR latent heating rate profiles

In general, the CFAD frequencies of the PR positive latent heating values are very comparable with the corresponding ELDORA derived values. For the case of the outer rainband in Jangmi, the normalized frequency contour lines larger values than 10^{-3}, 10^{-4}, and 10^{-5} have PR maximum heating values of 8 K h^{-1}, 20 K h^{-1}, and 50 K h^{-1}, while the corresponding ELDORA maximum heating values are 13 K h^{-1}, 25 K h^{-1} and 45 K h^{-1}, respectively (Fig. 2).

For the proposed TRMM-based study of tropical cyclone formations, the PR algorithm must also have some ability to distinguish dissimilar heating peaks between two outer rainbands. The CFADs for the PR latent heating rates for the Jangmi outer rainband Case I have a low-level heating maxima. By

contrast, those for Case II have upper-level maxima for most of profiles (contour line of 10^{-3}), which is consistent with the ELDORA retrievals. The PR algorithm also presents the different heating profiles between Case III and Case IV for their majority of the contours (e.g., contour line of 10^{-3}). In summary, relative changes in majorities of PR latent heating profiles can represent some indication of latent heating changes. However, the CFAD comparison between the PR and the ELDORA for an individual case shows systematic bias, so the current PR algorithm is not accurate enough to apply to meso-scale aspect of tropical cyclone formation studies to test the top down and bottom up theories.

The ELDORA-derived cooling rates have important structure and magnitude changesat different tropical cyclone stages. By contrast, the PR algorithm greatly underestimates the negative latent heating rates via evaporation cooling in every case. For the case of the outer rainband in Jangmi, the normalized frequency contour lines of 10^{-3}, 10^{-4}, and 10^{-5} from the PR have maximum cooling values of 1 K h^{-1}, 3 K h^{-1}, and 8 K h^{-1}, while the corresponding ELDORA maximum cooling values are 15 K h^{-1}, 30 K h^{-1} and 50 K h^{-1}, respectively (Fig. 2). A possible explanation for this significant underestimation of cooling is an inherent observational sensitivity difference between the two sensors. That is, PR is only sensitive to large ice particles (graupel) within the convective region due to its sensor frequency (13.8 GHz), and is not able to detect small particles mostly within the stratiform region and anvil of the MCS. The second explanation for the underestimate of cooling in the PR latent heating rate algorithm is that the look-up table based on cloud-resolving model simulations over the TOGA COARE region may reasonably represent cloud microphysics in the convective region of the MCS, but fail to simulate the stratiform and anvil region in strong vertical wind shear conditions.

c. *Implications for satellite algorithm development and mesoscale diagnosis*

This study makes a significant conclusion that estimating the three-dimensional latent heating and cooling profiles from the TRMM PR observations via a cloud-resolving model based look-up table is still very challenging. Shige et al. (2007) have shown that PR latent heating profile algorithm reasonably represents the latent heating maxima calculated using a rawinsonde sound-based method. Averaging latent heating profiles over wide areas (~ grid scale of cloud model) might have increased correlation between the profiles of the ELDORA and the PR algorithm. Nevertheless, the evaluation of the satellite algorithm is found to under-estimate the effect of evaporative cooling. Thus, an upgrade of the algorithm is required to represent evaporative cooling magnitudes and vertical profiles in tropical cyclone formation and intensification conditions.

REFERENCES

Roux, F., V. Marécel, and D. Hauser, 1993: The 12/13 January 1988 narrow cold-frontal rainband observed during MFDP/FRONTS 87. Part I: Kinematic and thermodynamics. *J. Atmos. Sci.*, **50**, 951–974.

Shige, S., Y. N. Takayabu, W.-K. Tao, and C.-L. Shie, 2007: Spectral retrieval of latent heating profiles from TRMM PR data. Part II: Algorithm improvement and heating estimates over tropical ocean regions. *J. Appl. Meteor.*, **43**, 1095–1113.

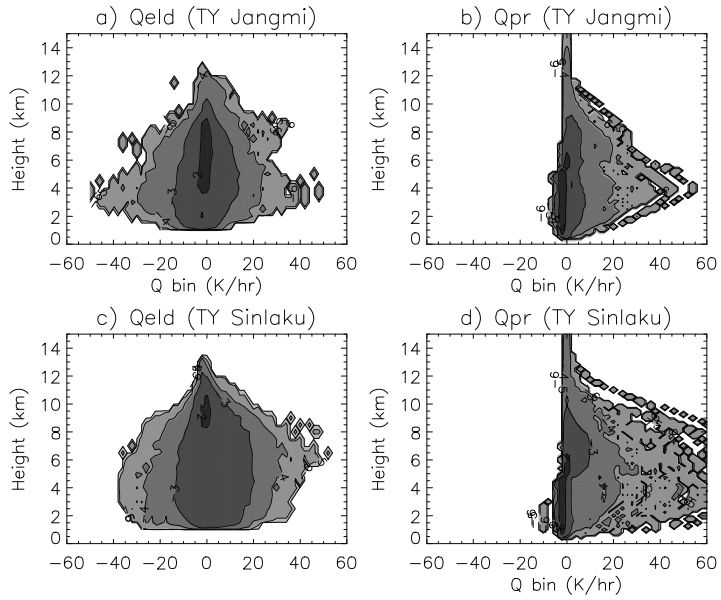

Figure 2. Contoured frequency by altitude diagrams (CFADs) of the ELDORA-derived latent heating rate and the PR-derived latent heating rate for two mature tropical cyclone circulations: Case I (Super TY Jangmi) in upper panel and Case II (TY Sinlaku) in lower panel. The frequencies are normalized by total non-missing number of each variable, and the shading ranges increase on a logarithmic scale. The contour line the exponent indicates x in the normalized frequencies of 10